

Optical Oxygen Sensors

UTILISING THE LUMINESCENCE OF PLATINUM METALS COMPLEXES

By Professor Andrew Mills

Department of Chemistry, University of Wales Swansea

Oxygen is an immensely important chemical species – essential for life. The need to determine levels of oxygen occurs in many diverse fields. In environmental analysis, oxygen measurement provides an indispensable guide to the overall condition of the ecology and it is routine practice to monitor oxygen levels continuously in the atmosphere and in water. In medicine, the oxygen levels in the expired air or in the blood of a patient are key physiological parameters for judging general health. Such parameters should ideally be monitored continuously, which may present problems. Determining oxygen levels in blood requires blood samples which may be difficult to take or impossible to take regularly – the elderly suffer from collapsed veins, while babies may only have 125 cm³ of blood. The measurement of oxygen levels is also essential in industries which utilise metabolising organisms: yeast for brewing and bread making, and the plants and microbes that are used in modern biotechnology, such as those producing antibiotics and anticancer drugs. Here, the background to oxygen measurements is described and work to develop new optical oxygen sensors which utilise the luminescence of platinum metals complexes is discussed.

Due to its widespread importance, the quantitative determination of oxygen, in the gas phase or dissolved in a liquid phase, is a cornerstone piece of analysis that has been dominated for the last three decades by electrochemical sensors, such as the amperometric Clark cell or the galvanic Mancy cell (1). These sensors are robust and quite reliable when used correctly. However, they are bulky and not readily miniaturised (without great expense); they also suffer from electrical interference and, since they consume oxygen, can easily generate misleading data. Thus, there is a constant interest in new, superior techniques for oxygen detection, and optical oxygen sensors represent one of the new hopefuls in this area (2, 3). Optical oxygen sensors are cheap, easily miniaturised and simple to use. Additionally, they do not suffer from electrical interference or consume oxygen. Optical sensors for other analytes, including pH (4), carbon dioxide (5) and biological analytes, such as glucose (6), have also been developed. By coupling optical sensors for a range of

analytes onto the distal end of a fibre optic it is possible to perform remote, non-perturbing, multianalyte analysis in very confined spaces, such as blood vessels (7).

Early Optical Oxygen Sensors and Their Basic Operating Principles

Most optical oxygen sensors respond specifically and usually reversibly to molecular oxygen by a change in the intensity of luminescence emitted from a probe molecule. The luminescence is reversibly quenched by molecular oxygen. The luminescent probe molecules are usually encapsulated in a gas permeable, but ion impermeable, material such as silicone rubber, to create the thin-film oxygen sensor.

The field of optical oxygen sensors is dominated by platinum metals complexes, which are used as the oxygen-quenchable lumophoric probe, and in particular by the following three luminescent platinum metals complexes:

- tris(4,7-diphenyl-1,10-phenanthroline)-ruthenium(II), represented by $[\text{Ru}(\text{dpp})_3]^{2+}$;

Table I
Photochemical Characteristics of the Ruthenium Complexes, [Ru(bpy)₃]²⁺, [Ru(phen)₃]²⁺ and [Ru(dpp)₃]²⁺ in Water*

Dye	Luminescence lifetime, τ_0 , μs	λ_{max} (absorption), nm	Molar absorptivity, $10^4 \text{ dm}^3 \text{ mol}^{-1} \text{ cm}^{-1}$	λ_{max} (emission), nm	Φ_{L} Quantum yield of luminescence	$k_{\text{d}}(\text{O}_2)$, $10^9 \text{ dm}^3 \text{ mol}^{-1} \text{ s}^{-1}$	$p\text{O}_2$ (S = 1/2) in silicone rubber, RTV 118, torr (8)	Refs.
[Ru(bpy) ₃] ²⁺	0.60	(423) _{sh} , 452	1.46	613, 627	0.042	3.3	376.8	9, 10, 11
[Ru(phen) ₃] ²⁺	0.92	447, 421	1.83, 1.90	605, 625	0.080 in 2-butanone	4.2	111.3	11, 12
[Ru(dpp) ₃] ²⁺	5.34 in methanol	460	2.95	613, 627	~ 0.30 in water/ethanol	2.5 in methanol	29.8	11, 13, 14

* unless stated otherwise

$k_{\text{d}}(\text{O}_2)$ is the bimolecular quenching rate constant of the electronically excited state of the luminescent dye by oxygen

sh is shoulder

- tris(1,10-phenanthroline)ruthenium(II), [Ru(phen)₃]²⁺ and
- tris(2,2'-bipyridyl)ruthenium(II), [Ru(bpy)₃]²⁺.

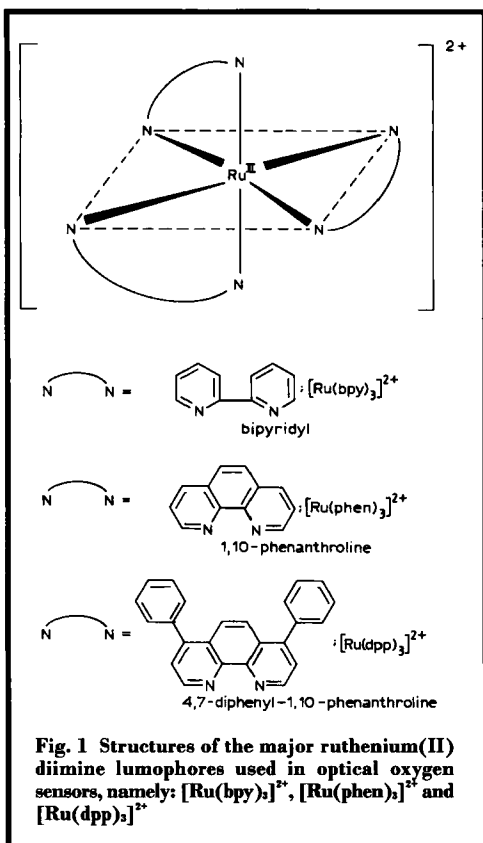
Their structures are illustrated in Figure 1. These are very photostable dyes with long excited-state lifetimes and high quantum yields of luminescence. They are readily quenched by oxygen, as indicated by the data in Table I. The longer lifetime of the [Ru(dpp)₃]²⁺ species has made it a particular favourite in recent attempts to develop optical oxygen sensors of greater sensitivity than earlier ones based on [Ru(bpy)₃]²⁺.

In an homogeneous medium, such as an aqueous solution, quenching the luminescence of ruthenium diimine complexes, including those in Figure 1, by oxygen has been found to obey the Stern-Volmer equation:

$$I_0/I = \tau_0/\tau = 1 + K_{\text{sv}} \cdot p\text{O}_2 \quad (\text{i})$$

where $I_0(\tau_0)$ and $I(\tau)$ are the intensities (lifetimes) of the luminescence in the absence and presence, respectively, of oxygen at partial pressure, $p\text{O}_2$, and K_{sv} is the Stern-Volmer constant. The Stern-Volmer constant depends directly upon the rate constant for the diffusion of oxygen, the solubility of oxygen and the natural lifetime of the electronically-excited state of the lumophore in the plastic medium. In much of the work on optical oxygen sensors, it is the intensities, I_0 and I , that are studied, rather than the lifetimes, τ_0 and τ . Certainly, in any commercial device incorporating such sensors it will be much simpler and cheaper to measure the intensities instead of the excited state lifetimes. Lifetime measurements however, have an advantage over intensity measurements, since they are not usually affected by processes which result in loss of the complex, such as leaching or photodegradation. Figure 2(a) illustrates the variation in the emission spectrum of [Ru(bpy)₃]²⁺ dissolved in water under atmospheres of nitrogen, air and oxygen.

In most of the luminescent oxygen sensors developed to-date, where the lumophore is incorporated into a polymer matrix, such as silicone rubber, it has been observed that, in contrast to homogeneous solutions, the Stern-Volmer plot of I_0/I versus $p\text{O}_2$ has a downward curvature.



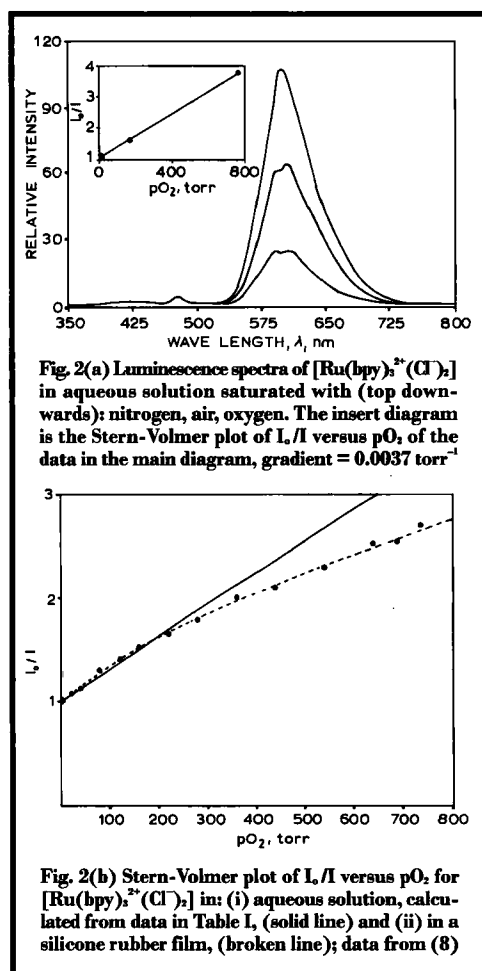
Two models: the multisite model and the non-linear solubility model, have been used to account for this phenomenon (8, 15). In the multisite model, it is suggested that the sensor molecule can exist at two or more sites, each with its own characteristic quenching constant. The non-linear solubility model assumes that deviation from linearity is due to the non-linear solubility of oxygen in the polymer. Both models predict the following modified form of the Stern-Volmer equation:

$$I_0/I = 1 + A.p\text{O}_2 + B.p\text{O}_2/(1 + b.p\text{O}_2) \quad (\text{ii})$$

where A, B and b are constants relating to the parameters in the kinetic and solubility equations associated with the respective models.

The above equation successfully fits the observed data associated with most optical oxygen sensors. Figure 2(b) shows the straight-line variation of I_0/I versus $p\text{O}_2$ for $[\text{Ru}(\text{bpy})_3]^{2+}$ in

aqueous solution, predicted from the data in Table I and Equation (i), and the downward-curving variation found when the same complex is encapsulated in silicone rubber. In the silicone rubber medium the Stern-Volmer plot is curved and less steep, indicating that it is generally less oxygen sensitive. This is a common feature of encapsulation, not usually due to a variation in the natural lifetime of the probe, which is largely unchanged on going from an aqueous medium to an encapsulating solid medium. Instead, it is due to a combination of a lower solubility of oxygen and a lower bimolecular quenching rate constant – the latter is usually diffusion controlled. A useful quick, though rough, guide to the sensitivity of any



oxygen optrode at low oxygen levels, is the value of the partial oxygen pressure, pO_2 , when the intensity of luminescence, I , has dropped to a value of $I_0/2$, that is $pO_2(S = 1/2)$. In an homogeneous medium, where quenching is expected to obey the Stern-Volmer equation (Equation (i)) the parameter $pO_2(S = 1/2)$ is given by:

$$pO_2(S = 1/2) = 1/K_{sv} \quad (\text{iii})$$

However, for the majority of optical oxygen sensors, the variation in luminescence as a function of pO_2 is more likely to be described by Equation (ii) – the modified form of the Stern-Volmer equation – and parameter $pO_2(S = 1/2)$ is described by the following expression:

$$pO_2(S = 1/2) = \frac{[-(A+B-b) \pm \sqrt{(A+B-b)^2 + 4Ab}]}{2Ab} \quad (\text{iv})$$

Table I lists the $pO_2(S = 1/2)$ values for the $[Ru(dpp)_3]^{2+}$, $[Ru(phen)_3]^{2+}$ and $[Ru(bpy)_3]^{2+}$ lumophores encapsulated as their perchlorate salts in silicone rubber. These results show that the most oxygen sensitive films of all the ruthenium(II) diimine complexes tested incorporate the $[Ru(dpp)_3]^{2+}$ species.

The common chloride and perchlorate salts of the ruthenium diimine complexes listed in Table I are hydrophilic and thus not readily soluble in the hydrophobic encapsulating polymer medium (8). Early optical oxygen sensors were made by soaking the silicone rubber in a dichloromethane solution of a hydrophilic luminescent salt, $[Ru(dpp)_3(ClO_4)_2]$. The silicone rubber swells up in dichloromethane and the ruthenium complex can then penetrate the film and become trapped after the highly volatile solvent evaporates (8). Such sensors still have problems, such as dye leaching and fogging, especially when exposed to humid air or aqueous solution, and low luminescence, due to the low solubility of the hydrophilic complex salt (8).

Work by us (16) and others (17, 18) has shown that hydrophilic cationic luminescent species, such as $[Ru(bpy)_3]^{2+}$, $[Ru(phen)_3]^{2+}$ and $[Ru(dpp)_3]^{2+}$, can be readily solubilised into a hydrophobic polymer medium, by coupling the cation with a hydrophobic anion, such as tetraphenyl borate or dodecyl sulfate, to

create a hydrophobic ion-pair, for example $[Ru(dpp)_3]^{2+}(Ph_4B^-)_2]$. Using this approach, a range of thin-film luminescence oxygen sensors can be produced with much greater stability to dye leaching and film fogging, and with better response times, luminescence intensities and stabilities than prior oxygen sensors. Table II describes some optical oxygen sensors based on the ruthenium diimine cations.

Tuning the Sensitivity of Optical Oxygen Sensors

The sensitivity of an optical oxygen sensor depends mainly upon the ability of oxygen to quench the luminescence emitted by the probe. This depends, in turn, upon:

- [a] The natural lifetime of the excited luminescent state in the absence of oxygen, τ_0 ; long lived excited states favour the creation of sensitive oxygen sensors.
- [b] The rate of diffusion and solubility of oxygen in the encapsulating medium; combining these two parameters is the permeability of the medium towards oxygen, and the greater this value the more sensitive the oxygen sensor.
- [c] The efficiency of quenching: the optimum situation is when the excited state of a luminescent probe molecule is quenched whenever it encounters an oxygen molecule, thus the process is diffusion-controlled. This is usually the case for most optical oxygen sensors.

Oxygen sensors with different sensitivities can be created by varying [a] to [c]. Factors [a] and [c] depend largely upon the nature of the luminescent probe dye. Thus, sensors of low sensitivity ($pO_2(S = 1/2) = 377$ torr) and high sensitivity ($pO_2(S = 1/2) = 29.8$ torr) towards oxygen have been made using the ruthenium diimine cations: $[Ru(bpy)_3]^{2+}$ ($\tau_0 = 0.6 \mu s$) and $[Ru(dpp)_3]^{2+}$ ($\tau_0 = 5.3 \mu s$), respectively (8), see Table I. The variation in sensitivity is primarily due to the difference in τ_0 of the two probe dyes.

Early Work with Silicone Rubber

It is also possible to alter the sensitivity of an optical oxygen sensor by using different encapsulating media which have different values for factor [b]. This is most dramatically illustrated

Table II Characteristics of Typical Ruthenium Dimine Oxygen Luminescent Sensors						
Luminescent Ion-Pair	Encapsulating Medium ^a	A, 0.001	B, 0.001	b, 0.001	pO ₂ (S = 1/2), torr ^b	Ref.
[Ru(bpy) ₃ ²⁺ (Ph ₄ B ⁻) ₂]	Cellulose acetate + TBP plasticiser (200 phr)	7.05	2.88	17.74	126	17
[Ru(bpy) ₃ ²⁺ (ClO ₄ ⁻) ₂]	Silicone with silica filler (RTV118; GE)	1.15	2.91	2.48	377	8
[Ru(bpy) ₃ ²⁺ (Cl ⁻) ₂]	Dye supported on kieselgel dispersed in silicone (E43; Wacker)	1.46	8.59	2.43	124	19
[Ru(phen) ₃ ²⁺ (ClO ₄ ⁻) ₂]	Silicone with silica filler (RTV118; GE)	3.94	10.14	9.03	111	8
[Ru(phen) ₃ ²⁺ (Cl ⁻) ₂]	Dye supported on kieselgel dispersed in silicone (E43; Wacker)	13.83	4.49	4.22	57.3	6
[Ru(dpp) ₃ ²⁺ (Ph ₄ B ⁻) ₂]	PMMA + TBP plasticiser (133 phr)	15.0	29.0	5.63	28.0	16
[Ru(dpp) ₃ ²⁺ (DS ⁻) ₂]	Silicone (E43; Wacker)	5.39	20.18	9.93	54.0	12
[Ru(dpp) ₃ ²⁺ (ClO ₄ ⁻) ₂]	Silicone with silica filler (RTV118; GE)	21.95	12.28	1.92	29.8	8
[Ru(dpp) ₃ ²⁺ (ClO ₄ ⁻) ₂]	Silicone with silica filler (RTV118; GE)	35.05	25.47	15.88	18.3	20
[Ru(dpp) ₃ ²⁺ (ClO ₄ ⁻) ₂]	Silicone (RTV 732; Dow Corning)	12.96	20.33	4.52	32.6	15
[Ru(dpp) ₃ ²⁺ (ClO ₄ ⁻) ₂]	Polystyrene	1.28	1.15	1.13	495	21
[Ru(dpp) ₃ ²⁺ (ClO ₄ ⁻) ₂]	Polyvinylchloride	6.30	1.46	3.92	138	22
[Ru(dpp) ₃ ²⁺ (Cl ⁻) ₂]	Silicone (RTV 732; Dow Corning)	1.93	47.19	20.98	33.9	23

^a Unless stated otherwise all silicones referred to here were generated from one-component, acetic acid releasing, silicone prepolymer with no added silica filler; phr = parts per hundred resin

^b Most oxygen optical sensors give Stern-Volmer plots (I₀/I versus pO₂) which deviate from linearity and obey Equation (ii). For each oxygen sensor the original data reported in the associated article were fitted to the modified Stern-Volmer equation, Equation (ii) and the values for A, B and b, which provide the optimum fit, were used to calculate the values for pO₂(S = 1/2) reported in this Table using Equation (iv). All the oxygen sensors referred to in this Table are the most sensitive for which Stern-Volmer data were given in the associated article

by the results in Table III, which lists the oxygen sensitivities, as measured by the value of pO₂(S = 1/2) for a series of films of [Ru(dpp)₃²⁺(Ph₄B⁻)₂] encapsulated in different polymers; the lower the value of pO₂(S = 1/2) the greater the oxygen sensitivity of the sensor. Silicone rubber is clearly preferred as the encapsulating medium, see Table II. This is because silicone rubber has very high permeability, 100 times greater than for any other organic polymer (26), high chemical and mechanical stability, and it is very hydrophobic. The latter minimises dye leaching and interference quenching by any ionic species in the test medium.

Although different commercial silicone rubbers have been used as the encapsulating medium, it is not always clear which characteristics of the final cured encapsulating medium determine the overall sensitivity of the resultant oxygen sensor. The situation is complicated by the proprietary nature of the silicone rubbers – some commercial silicone rubber formulations have added silica filler, full details of which are not readily available. Elegant work carried out by Demas and co-workers has demonstrated that the presence of silica in a silicone rubber can considerably alter the sensitivity of the oxygen sensor (27).

Plasticised Polymers

At present, tuning the sensitivity of an oxygen sensor which utilises silicone rubber is often crude, empirical and lacking in dynamic range. However, unlike silicone rubber, polymers such as

Encapsulating polymer	A, 10^{-3}	B, 10^{-3}	b, 10^{-3}	$p\text{O}_2$ (S = 1/2), torr	Ref.
Silicone rubber	21.9	12.3	1.92	29.8	8
Cellulose acetate	0.0376	3.27	0.594	368	24
Polymethyl methacrylate	0.199	1.61	0.683	806	16
Polyvinyl chloride	–	–	–	> 1000	25

cellulose acetate (CA), polymethyl methacrylate (PMMA) and polyvinyl chloride (PVC) can be obtained in a well defined, reproducible form. As shown in Table III, such polymers have poor oxygen diffusion/solubility characteristics and are of limited use by themselves as the encapsulating medium. However, these three polymers are also readily plasticised, with such species as tributyl phosphate (TBP) and dioctyl phthalate, to create films which have much better oxygen diffusion/solubility characteristics than the pure polymer (28). As a result, plasticisation of a polymer encapsulating medium, such as CA, PMMA or PVC, with TBP for example, allows the sensitivity of an optical oxygen sensor to be increased markedly in a well-defined manner.

The variation in the Stern-Volmer plots for a series of $[\text{Ru}(\text{dpp})_3^{2+}(\text{Ph}_4\text{B}^-)_2]$ in PMMA films

which contain increasing amounts of TBP plasticiser is shown in Figure 3. The sensitivity of the optical oxygen film increases with plasticisation, and so do the 90 per cent response and recovery times of the film, when exposed to an alternating atmosphere of 100 per cent oxygen (response) and nitrogen (recovery). This is shown in Figure 4 for the same series of films of $[\text{Ru}(\text{dpp})_3^{2+}(\text{Ph}_4\text{B}^-)_2]$ in PMMA.

Plasticisation of a polymer increases its workability, flexibility and distensibility and, most importantly for the oxygen optical films, the mobility of polymer segments. The latter leads to an increase in gas diffusion coefficients (17). It is common practice to refer to the value of the solubility parameter, δ , of the plasticiser and the polymer in order to identify compatible plasticiser-polymer combinations.

In general, it has been suggested that the

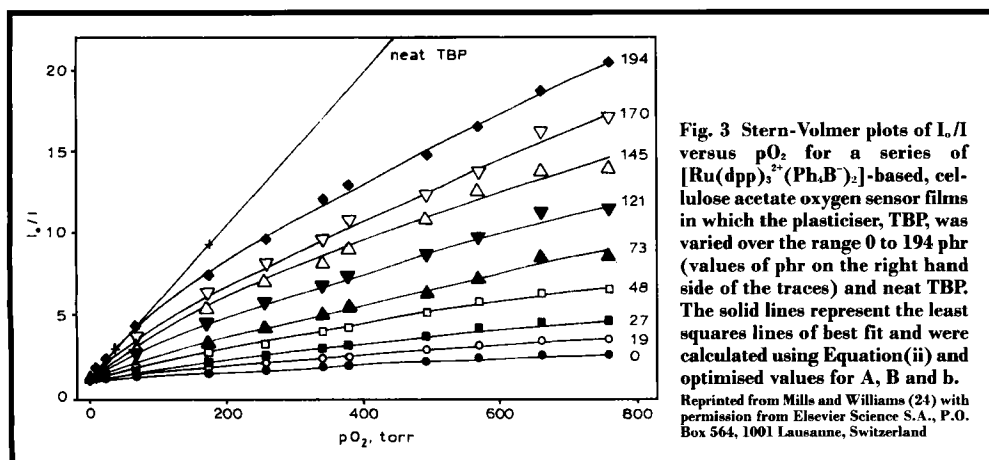
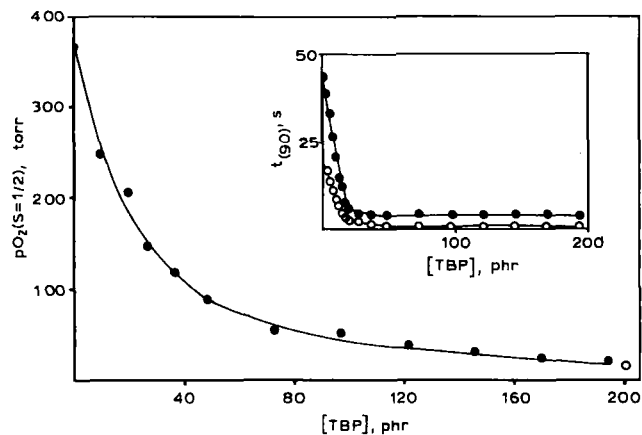


Fig. 4 Plot of $pO_2(S = 1/2)$ versus TBP concentrations derived from data shown in Figure 3 for the $[Ru(dpp)_2^{2+}(Ph_4B^-)_2]$ -based, cellulose acetate oxygen sensor films, containing different amounts of plasticiser. The (o) point represents the value for $pO_2(S = 1/2)$ obtained for the dye dissolved in neat TBP plasticiser. The insert diagram shows the observed variation in the 90 per cent response (open circles) and recovery (black circles) times, $t_{(90)}$, recorded for the films. Data from (24); phr = parts per hundred resin (weight per cent of plasticiser with respect to the polymer)



difference in these solubility parameters:

$$\{\Delta\delta = \delta(\text{polymer}) - \delta(\text{plasticiser})\}$$

should be less than $3.7 \text{ (J cm}^{-3}\text{)}^{1/2}$ (29). Table IV lists the solubility parameters and $\Delta\delta$ values for a series of films of polymers plasticised with TBP ($\delta = 17.5 \text{ (Jcm}^{-3}\text{)}^{1/2}$) containing $[Ru(dpp)_2^{2+}(Ph_4B^-)_2]$. From the values of $pO_2(S = 1/2)$, determined for the corresponding $[Ru(dpp)_2^{2+}(Ph_4B^-)_2]$ -in-polymer-plasticised-with-TBP (30 phr) films, it appears that, in general, the greater the polymer-plasticiser compatibility, that is the smaller $\Delta\delta$, the greater is the oxygen sensitivity of the film. The latter observation is not surprising given that the sensitivity of the optical oxygen film sensor depends on both the rate constant for the diffusion of oxygen through the film and also the solubility of oxygen in the film. Both of these parameters are expected to improve with plasticisation.

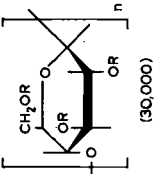
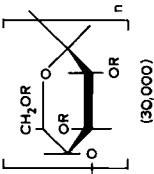
Optical Oxygen Sensors Based on Platinum Metals Porphyrins

Much of the early work on optical oxygen sensors was driven by their possible medical use; in particular, as part of the development of remote, cheap, continuous bedside monitoring of a patient's condition. The oxygen levels that were of interest centred on the amount in air, namely 159 torr or 21 per cent and the ruthenium(II) diimine complexes, when encapsulated in silicone rubber or a plasticised polymer,

are quite well suited for operating at or around this level. However, as optical oxygen sensors have developed, interest in them has grown together with a realisation that more sensitive ones could find application elsewhere. One example is in modified-atmosphere food packaging; many foods, especially meats, are packaged in the absence of oxygen to minimise bacterial growth. Carbon dioxide is usually the packaging gas, but vacuum packaging is commonplace for supermarket foods. Therefore the incorporation of a cheap, disposable optical oxygen sensor as a label in the packing, which would operate at, say, the 15 torr, 2 per cent oxygen level, would provide an ideal check that the packaging is intact. Other possible areas of application are in the control of anaerobic processes and low vacuums.

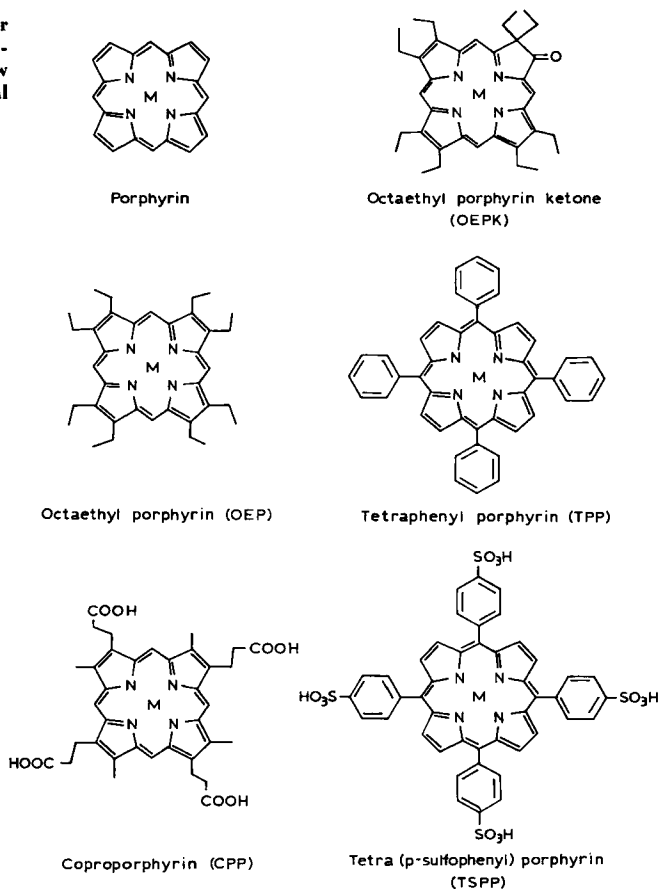
The development of more sensitive optical oxygen sensors has been dominated by the use of platinum metals porphyrins as the luminescent probes. Such probes absorb and emit light in the visible spectrum (typically, at 540 nm and 655 nm, respectively) have long excited state lifetimes (usually $> 10 \mu\text{s}$) and in many cases are commercially available. Some of the platinum metals porphyrin structures used as luminescent probes in optical oxygen sensors are shown in Figure 5; invariably the metal in such complexes is platinum or palladium.

Porphyrins of platinum and palladium do not usually fluoresce, rather they phosphoresce and

Table IV Characteristics of Some Different Polymers Used to Create [Ru(dpp) ₃ (Ph ₄ B) ₂] Films of Different Oxygen Sensitivity, Plastified with TBP (30 phr)								
Polymer	Abbreviation	Molecular formula (Molecular weight)	Solubility parameter, δ , (J cm ⁻³) ^{1/2}	Oxygen sensitivity characteristics of [Ru(dpp) ₃ (Ph ₄ B) ₂] in films comprising different polymers, plastified with TBP (30 phr)			$\Delta\delta$, (J cm ⁻³) ^{1/2}	
				A, 10 ⁻³	B, 10 ⁻³	b, 10 ⁻³		pO ₂ (S = 1/2), torr
Cellulose acetate butyrate	CAB	 (30,000)	17.9	6.53	6.30	4.94	92	0.4
Cellulose acetate	CA	 (30,000)	17.9	0.0115	7.49	0.655	146	0.4
Poly(vinyl acetate)	PVAc	(-CH ₂ CH(O ₂ CCH ₃)-) _n (113,000)	19.1	3.07	4.34	7.31	209	1.6
Polystyrene	PS	(-CH ₂ CH(C ₆ H ₅)-) _n (45,000)	18.5	2.53	5.93	11.5	245	1.0
Poly(methyl methacrylate)	PMMA	(-CH ₂ C(CH ₃)(CO ₂ CH ₃)-) _n (120,000)	18.8	2.27	6.29	16.3	300	1.3
Poly(methyl methacrylate)	PMMA	(-CH ₂ C(CH ₃)(CO ₂ CH ₃)-) _n (33,800)	18.8	2.47	2.72	8.09	308	1.3
Poly(vinyl chloride)	PVC	(-CH ₂ CH(Cl)-) _n (95,000)	19.2	1.53	1.90	4.15	457	1.7

For CAB: R = -COCH₃ or -COCH₂CH₂CH₃; for CA: R = -COCH₃ or H; $\Delta\delta$ = δ (polymer) - δ (plasticiser)

Fig. 5 Structures of the major platinum and palladium porphyrins used to create the new range of very sensitive optical oxygen sensors; see Table V



this lack of any short-lived fluorescence is an advantage over many other long-lived phosphorescent species, such as polycyclic aromatics, since it reduces the problems associated with background interference. Most of the platinum metals porphyrin optical oxygen sensors reported to-date are shown in Table V; unless stated otherwise the encapsulating medium is homogeneous, that is no plasticisers are included. It can be seen that the non-quenched, natural, lifetimes, τ_0 , of the platinum and palladium porphyrins differ by about an order of magnitude and, as a result, any such pair of porphyrin probes allows a considerable range of oxygen concentrations to be covered.

Unlike the ruthenium(II) diimine complexes, the excited states of the platinum and palladium

porphyrins are much longer lived, typically many tens of microseconds for platinum porphyrins and many hundreds of microseconds for palladium porphyrins; see the lifetime data in Tables I and V. As a consequence, when the platinum metals porphyrins are incorporated into the same polymer media used for the ruthenium diimine optical oxygen sensors, the resultant sensors are more oxygen sensitive. This can be seen by comparing the $pO_2(S = \frac{1}{2})$ values for the ruthenium(II) complexes listed in Tables II and III with those for the platinum and palladium porphyrins, listed in Table V. For example, the most oxygen sensitive of the ruthenium(II) complexes, $[Ru(dpp)_3^{2+}(Ph_4B^-)_2]$, when incorporated into non-plasticised PVC, produces a very oxygen insensitive film with $pO_2(S = \frac{1}{2}) > 1000$ torr,

Table V

Platinum and Palladium Porphyrin Based Optical Oxygen Sensors

Probe	τ_o , ms	λ (emission), nm & (ϕ_e) (32, 33, 39)	Medium	$pO_2/S = 1/2$, $1/K_{sv}$, torr	Comments	Ref.
Pd-CPP	0.40	667 (0.2) ¹⁶	water	0.535		30
Pd-CPP	0.80	667 (0.2) ¹⁶	silicone rubber RTV 118(GE)	3.57	A lifetime study, including an investigation of the effects of temperature, ageing and possible interferants, such as nitrous oxide and carbon dioxide. This silicone rubber is a clear, one component, acetic acid releasing prepolymer, with an unspecified amount of silica filler	31
Pd-CPP	1.06	667 (0.2) ¹⁶	PS	7.2		
Pd-CPP	0.91	667 (0.2) ¹⁶	PMMA	27.1		32
Pt-OEPK	0.061	760 (0.1) ⁹	PS	49.2		
Pt-OEPK	0.061	759 (0.12)	PS	56.9	The $1/K_{sv}$ value here was calculated from $\tau_o = 61.4 \mu s$ and $\tau_{oR} = 16.3 \mu s$. The Pt-OEPK is tens of times more photostable than Pt-OEP	33
Pt-OEPK	0.058	759 (0.12)	PS	32	Also encapsulated in PVC although the films are not as sensitive	34
Pd-OEPK	0.46	790 (0.01)	PS	5.6	Although a K_{sv} value of 0.189 torr^{-1} is reported in Table I of this ref. it is 10 times too big, as shown by the Stern-Volmer plot (Fig. 2(b), Ref. 34) of the original data for the film - we thank the authors for confirming this. The value for $1/K_{sv}$ reported here was calculated from the latter data	
Pt-OEPK	0.064	759 (0.12) ¹⁰	PVC	685		
Pd-OEPK	0.44	790 (0.01)	PVC	89.3		
Pd-TTP	-	690	Arachidic acid Langmuir-Blodgett film	2.58		35
Pd-TSPP	1.0	702 and 763	water	0.45	k_a for oxygen = $1.3 \times 10^5 \text{ dm}^3 \text{ mol}^{-1} \text{ s}^{-1}$	36
Pd-TSPP	0.5	698; 685	water	0.40	k_a for oxygen = $2.9 \times 10^5 \text{ dm}^3 \text{ mol}^{-1} \text{ s}^{-1}$; addition of bovine serum albumin lowers the oxygen sensitivity by a factor of 3.6	37
Pd-CPP	0.53	667	water	0.29	k_a for oxygen = $3.8 \times 10^5 \text{ dm}^3 \text{ mol}^{-1} \text{ s}^{-1}$; addition of bovine serum albumin lowers the oxygen sensitivity by a factor of 17	
Pt-TDCPP	0.082	650 (0.16)	Silicone rubber	8.0	The silicone rubber is a clear, one-part polymer, with no filler; all sensors covered by a Teflon [®] membrane. All Stern-Volmer plots show downward curvature; halogenation improves photostability of porphyrin sensors	38
Pt-TFMPP	0.030	646 (0.08)	RTV 732	3.7		
Pt-B ₁₀ TMP	0.023	721 (0.02)	RTV 732	6.4		
Pd-OEP	0.99	670 (0.2)	PS	-		32
Pt-OEP	0.091	644 (0.5)	PS	53.9	$\tau_{air} = 23 \mu s$	
Pt-OEP	0.091	644 (0.5) ⁹	PS	0.481	The $1/K_{sv}$ value was calculated from the Stern-Volmer plot (Fig. 6) in the reference in which the x-axis (P _{air}) is almost certainly mislabelled 0-1 kPa, where it should be 0-100 kPa, giving a $1/K_{sv}$ value of 54 torr, consistent with later work by the author (32)	39

CPP: coproporphyrin; OEPK: octaethyl porphyrin ketone; TTP: tetraphenylporphyrin; TSPP: tetraakis(4-sulfonatophenyl) porphyrin; TDCPP: meso-tetra(2,6-dichlorophenyl)porphyrin; TFMPP: meso-tetra(3,5-bis(trifluoromethyl)phenyl)porphyrin; B₁₀TMP: meso-tetramethyl- β -octabromoporphyrin; OEP: octaethyl porphyrin

Table III. On the other hand, when platinum and palladium octaethylporphyrin ketones (Pt-OEPK and Pd-OEPK) are incorporated into non-plasticised PVC the oxygen sensors are much more sensitive, $pO_2(S = 1/2)$ are 685 and 89.3 torr, respectively, see Table V. Indeed, Pd-OEPK in non-plasticised PVC is almost as sensitive as $[Ru(dpp)]^{2+}$ in silicone rubber, or highly plasticised PMMA (Table II).

Interestingly, the platinum and palladium porphyrins do not usually display non-linear, downward-curving Stern-Volmer plots; thus the pO_2 ($S = 1/2$) values reported in Table V have been calculated using Equation (iii); whereas those in Table II have been calculated using Equation (iv). Presumably, linear Stern-Volmer plots associated with the platinum and palladium porphyrin sensors indicate that the platinum and palladium porphyrins largely locate in the hydrophobic parts of the polymer, whereas the ruthenium diimine complexes can be found in different regions of the film, which thus exhibits multisite quenching behaviour. Optical oxygen sensors based on platinum and palladium octaethylporphyrins do show some evidence of multisite quenching at high levels of quenching ($L/I > 20$) if a plasticiser is added to the polymer encapsulating medium, although the effect is not very marked (34).

As with the ruthenium diimine complexes, the effect of plasticisation of the encapsulating polymer on the sensitivity of the platinum and palladium porphyrin optical oxygen sensors is dramatic, see Figure 6, which shows a plot of pO_2 ($S = 1/2$) versus [plasticiser] for a platinum octaethyl porphyrin ketone complex in a PVC sensor, using bis(2-ethylhexyl) sebacate as the plasticiser. This plot was generated using the results of Hartmann and Tretznak (34). Again, it is likely that the plasticiser improves the sensitivity of the sensor by improving the permeability of oxygen in the film.

Optical Biosensors and Future Opportunities

The growing interest in optical biosensors makes it likely that many more platinum metals complexes will be synthesised and tested for their

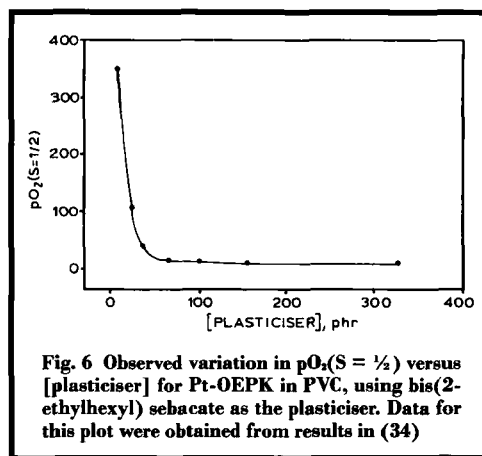


Fig. 6 Observed variation in $pO_2(S = 1/2)$ versus [plasticiser] for Pt-OEPK in PVC, using bis(2-ethylhexyl) sebacate as the plasticiser. Data for this plot were obtained from results in (34)

potential as quenchable lumophores in optical oxygen sensors. Optical biosensors have great potential for exploitation, and are another major application which is just beginning to be explored.

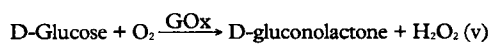
In a biosensor, a biochemical analyte is commonly detected using an enzyme to mediate a reaction between the analyte and a simple chemical species, such as oxygen, to generate simple chemical species, such as hydrogen peroxide, protons, carbon dioxide or ammonia. The level of the biochemical analyte is then determined from the steady-state concentration of one of the chemical species involved in the enzymatic reaction. Thus, a typical biosensor may simply be an enzyme layer covering an appropriate analytical device, such as a Clark electrode (for measuring oxygen) or a pH electrode. Since optical oxygen sensors offer a real challenge to Clark cells for the measurement of dissolved or gas phase oxygen levels, it appears likely that they may also be used in biosensor technology.

The glucose biosensor, for instance, is one of the simplest and most studied biosensors, and the measurement of glucose levels in clinical analysis is essential for the diagnosis of diabetes (40). The measurement of glucose levels is also needed for process control in a number of biotechnology and food industries.

In a typical glucose biosensor, the enzyme glucose oxidase (GOx) is used to mediate the

Table VI Oxygen-Consuming Biochemical Analyte/Enzyme Combinations	
Biochemical Analyte	Enzyme
Glucose	Glucose oxidase
Lactate	Lactate mono-oxygenase; Lactate oxygenase
Cholesterol	Cholesterol oxidase
Ascorbate	Ascorbate oxidase
Bilirubin	Bilirubin oxidase
Ethanol	Ethanol oxidase
Uric acid	Uricase
Penicillin	Penicillinase
Glutamate	Glutamate decarboxylase; Glutamate oxidase
Xanathine	Xanathine oxidase

reaction between glucose and oxygen, resulting in measurable products:



The level of glucose in a test medium can thus be determined from measurements of:

- [i] the production of hydrogen peroxide
- [ii] the production of gluconic acid, into which D-gluconolactone is rapidly converted, causing a drop in pH
- [iii] the consumption of oxygen.

Many types of glucose biosensors have been developed to measure [i] to [iii]. However, most utilise an electrochemical transducer and suffer from the usual problems of electrochemical sensors, such as being bulky, expensive and prone to electrical interference. Not surprisingly, in recent years fibre optical glucose biosensors have begun to be developed. Most work has been carried out using one of the ruthenium (II) diimine complexes in Table I as the optical oxygen sensor for the enzyme catalysed consumption of oxygen by glucose (41, 42). Such sensors are cheap, reliable, disposable, robust and easily miniaturised.

There is also a range of oxygen consuming biochemical analyte/enzyme combinations, for which an extensive number of different electrochemical biosensors has already been developed; Table VI lists some of the more popular oxygen-consuming analyte/enzyme combinations. Given the physiological importance of many of these biochemical analytes, it seems likely that optical biosensors, using platinum metals complexes as the transducers, will be an active area of research and development over the next few years.

Conclusions

Platinum metals complexes, such as ruthenium (II) diimines or platinum and palladium porphyrins, are playing a leading role in the new and promising area of optical oxygen sensors. Such sensors are expected to have a widespread impact on many fields, including medicine, environmental studies and in the biotechnology industries. The utilisation of these sensors for biosensing appears likely in the near future, although this remains, as yet, a still relatively unexplored area.

References

- 1 M. L. Hitchman, "Measurement of Dissolved Oxygen", John Wiley, Geneva, 1978, Ch. 1
- 2 W. R. Seitz, *CRC Crit. Rev. Anal. Chem.*, 1988, **19**, 135
- 3 O. S. Wolfbeis, in "Fiber Optic Chemical Sensors", ed. O. S. Wolfbeis, Vol II, CRC Press, Boca Ranton, FL, 1991, Ch. 10
- 4 J. I. Peterson and G. G. Vurek, *Science*, 1984, **224**, 123
- 5 A. Mills, Q. Chang and N. McMurray, *Anal. Chem.*, 1992, **88**, 1383
- 6 M. C. Moreno-Bondi, O. S. Wolfbeis, M. J. P. Leiner and B. P. H. Schaffar, *Anal. Chem.*, 1990, **62**, 2377
- 7 L. Li and D. R. Walt, *Anal. Chem.*, 1995, **67**, 3746
- 8 K. R. Carraway, J. N. Demas, B. A. DeGraff, and J. R. Bacon, *Anal. Chem.*, 1991, **63**, 337

- 9 C.-L. Lin and N. Sutin, *J. Phys. Chem.*, 1976, **80**, 97
- 10 J. van Houten and R. J. Watts, *J. Am. Chem. Soc.*, 1976, **98**, 4853
- 11 C.-T. Lin, W. Bottcher, M. Chou, C. Creutz and N. Sutin, *J. Am. Chem. Soc.*, 1976, **98**, 6536
- 12 I. Klimât and O. S. Wolfbeis, *Anal. Chem.*, 1995, **67**, 3160
- 13 J. N. Demas, E. W. Harris and R. P. McBride, *J. Am. Chem. Soc.*, 1977, **99**, 3547
- 14 K. Nakamaru, K. Nishio and H. Nobe, *Sci. Rep. Hiroaki Univ.*, 1979, **26**, 57
- 15 X.-M. Li, F.-C. Ruan and K. Y. Wang, *Analyst*, 1993, **118**, 289
- 16 A. Mills and M. Thomas, *Analyst*, 1997, **122**, 63
- 17 H. N. McMurray, P. Douglas, C. Busa and M. S. Garley, *J. Photochem. Photobiol.*, 1994, **80**, 283
- 18 I. Klimant and O. S. Wolfbeis, *Anal. Chem.*, 1995, **67**, 3160
- 19 O. S. Wolfbeis, M. J. P. Leiner, H. E. Posch, *Mikrochim. Acta*, 1986, **111**, 359
- 20 J. R. Bacon and J. N. Demas, *Anal. Chem.*, 1987, **59**, 2780
- 21 P. Hartmann, M. J. P. Leiner and M. E. Lippitsch, *Anal. Chem.*, 1995, **67**, 88
- 22 C. Preininger, I. Klimant and O. S. Wolfbeis, *Anal. Chem.*, 1994, **66**, 1841
- 23 B. Vojnovic, E. Blackwood, M. Grundon, R. J. Locke, R. G. Newman, G. West and W. K. Young, in "The Gray Laboratory Research Report 1995", The Gray Laboratory Research Trust, Mount Vernon Hospital, Middlesex, U.K., 1995, p. 31
- 24 A. Mills and F. Williams, *Thin Solid Films*, accepted for publication (MS No.: E-2170)
- 25 A. Mills and L. Monaf, manuscript in preparation
- 26 J. Brandrup and E. H. Immergut, eds., "The Polymer Handbook", 3rd Edn., Wiley, New York, 1989, p. VI/435
- 27 W. Xu, R. C. McDonough, B. Langsdorf, J. N. Demas and B. A. DeGraff, *Anal. Chem.*, 1994, **66**, 4133
- 28 J. Crank and G. S. Park, "Diffusion in Polymers", Academic Press, London, 1968, p. 21
- 29 R. B. Seymour and C. E. Carrher, "Polymer Chemistry – An Introduction", Marcel Dekker, New York, 3rd Edn., 1992, p. 394
- 30 P. M. Gewehr and D. T. Delpy, *Med. Biol. Eng. Comput.*, 1993, **31**, 2
- 31 P. M. Gewehr and D. T. Delpy, *Med. Biol. Eng. Comput.*, 1993, **31**, 11
- 32 D. B. Papkovsky, *Sens. Actuators B*, 1995, **29**, 213
- 33 D. B. Papkovsky, *Anal. Chem.*, 1995, **67**, 4112
- 34 P. Hartmann and W. Trettnak, *Anal. Chem.*, 1996, **68**, 2615
- 35 R. B. Beswick and C. W. Pitt, *Chem. Phys. Lett.*, 1996, **143**, 589
- 36 A. Harriman, *Platinum Metals Rev.*, 1990, **34**, (4), 181
- 37 J. M. Vanderkooi, G. Maniara, T. J. Green and D. F. Wilson, *J. Biol. Chem.*, 1987, **262**, 5476
- 38 W. W.-S. Lee, K.-Y. Li, Y.-B. Leung, C.-S. Chan and K. S. Chan, *J. Mater. Chem.*, 1993, **3**, 1031
- 39 D. B. Papkovsky, *Sens. Actuators B*, 1993, **11**, 293
- 40 T. J. Ohara, *Platinum Metals Rev.*, 1995, **39**, (2), 54
- 41 Z. Rosenzweig and R. Kopelman, *Anal. Chem.*, 1995, **67**, 2650
- 42 L. Li and D. R. Walt, *Anal. Chem.*, 1995, **67**, 2650

Platinum Nanorods in Carbon Nanotubes

Nanosized carbon tubes filled with metal are predicted to have many industrial applications, as catalysts, nanowires for conducting electricity and as composite materials. The preparation and structure of the carbon nanotubes and the encapsulated metal determine the form that the active metal will take. Indeed, metal may be deposited upon the nanotubes as well as inside them. One method commonly used to prepare carbon nanotubes is arc-discharge evaporation, with metal subsequently inserted into the nanotubes.

Now, researchers at Tohoku University, Japan, have prepared uniform platinum-filled carbon nanotubes, with metal deposited only within channels, by a template method using the electro-oxidation of aluminium plate (T. Kyotani, L.-F. Tsai and A. Tomita, *Chem. Commun.*, 1997, (7), 701–702). The resulting aluminium oxide film template was an array of parallel, straight channels of nanometre-scale diameter. Carbon was deposited on the channel walls by

thermal decomposition of propene. Platinum was loaded on this carbon film by impregnating with an ethanol solution of hexachloroplatinic acid at room temperature. The chloroplatinic acid was then reduced to platinum in the channels by either heat treatment at 500°C under hydrogen or by stirring with excess NaBH₄ solution at room temperature. The template was then removed with hydrofluoric acid and a platinum metal/carbon nanotube composite was obtained.

TEM images of composites prepared at 500°C showed the presence of uniform nanotubes with outer diameter and wall thickness of 30 nm and ~5 nm, respectively. Some tubes were filled with platinum nanorods (some >1 µm long) of high crystallinity (~300 nm), more abundant at the open tube ends. Room temperature reduction produced mostly platinum crystallites (2–5 nm). Thus platinum within these carbon nanotubes may be prepared either as nanorods or nanoparticles and their length, diameter and thickness are controllable and are monodisperse.